Supplementary Material – Learning Optimal K-space Acquisition and Reconstruction using Physics-Informed Neural Networks

Wei Peng[1,3] Li Feng[2] Guoying Zhao[1,*] Fang Liu[3,*]
[1]CMVS, University of Oulu [2]Icahn School of Medicine at Mount Sinai [3]Harvard Medical School

1. Implementation details

Our proposed models were designed using PyTorch [1] deep learning package. As shown in Figure 1 (a), the neural ODE uses a fully connected network (FCN) consisting of two fully connected layers and a Tanh activation function. The k-space location (*i.e.*, [kx, ky] in 2D acquisition) of the sampling points were concatenated together for all shots and used as the input of the FCN. The output size kept the same as the input. As shown in Figure 1 (b), like many medical image reconstruction studies, a U-Net [3] was used as the end-to-end reconstruction network to remove the residual artifacts and noises in the intermediate images, obtained using nuFFT and adjoint nuFFT operations on the optimized k-space trajectories. The U-Net structure comprises an encoder network with four layers of the down-sampling channel and a decoder network with a mirrored and reversed encoder structure. Multiple skip connections are used to concatenate entire feature maps from encoder to decoder to enhance mapping performance. In addition, because of the GPU memory limit, the multi-channel images were combined into one image using a root-sum-of-squares reconstruction (RSS) [2] and then used as the input of the U-Net network.

2. More Results

We provide qualitative comparisons with PILOT [6] under the same protocol. Here, we only use 1000 sampling points for each spoke. As shown in Table 1, our method can be much better especially when acceleration is high. As PILOT optimizes the acquisition by directly introducing a learnable matrix, which is surely sensitive to initialization and would easily stuck in suboptimal points.

As well, the learned k-space trajectories using Cartesian, and spiral trajectory as the initial sampling pattern were demonstrated in Figures 2, and 3, respectively. The Cartesian imaging uses straight-line sampling pattern to acquire k-space. In Figure 2, the learned trajectory uses a Cartesian trajectory as an initial sampling pattern. A wavy sampling pattern was formed at the canter region of each phase encoding line, becoming more efficient in acquiring the high-density k-space region than a straight line. Spiral imaging uses a curved sampling pattern to acquire k-space. In Figure 3, the spiral trajectory was further optimized to cover the k-space more efficiently. The initial uniform density spiral spoke adaptively concentrated into the central k-space region with a slightly wavy pattern, which assembles the variable density spiral sampling, which was previously shown to be more efficient in spiral imaging [5].

Table 1. Comparisons on brain AXT1 images, using radial.

Acc. Level	PILOT		Ours	
	PSNR	SSIM	PSNR	SSIM
16-shots	28.62 ± 0.66	0.77 ± 0.01	$\mathbf{31.03 \pm 0.59}$	$\mathbf{0.82 \pm 0.01}$
32-shots	31.24 ± 0.61	0.83 ± 0.01	$\mathbf{33.06 \pm 1.23}$	$\mathbf{0.86 \pm 0.01}$

The influence of the physical constraints on the optimized trajectories is also demonstrated in the middle of Figures 2, and 3. While the unconstrained trajectories attempted to rapidly explore large sampling space for covering more k-space information, the resulted trajectories tend to traverse with abrupt turns, leading to irregular non-smooth sampling patterns which are difficult to be implemented in MRI scanners. However, the learned trajectories under physical constraints can produce a hardware-friendly waveform for practical implementation.

The point-spread function (PSF) is also demonstrated for each corresponding trajectory in Figures 2, and 3. Compared with the fixed PSF, the learned trajectory can lead to a PSF with reduced side lobes and more homogeneous sampling of the neighboring pixels. This can result in reduced structural and aliasing imaging artifacts in the undersampled images.

The reconstructed images from the learned trajectories using Cartesian, and spiral trajectories were demonstrated in Figures 4, and 5, respectively. These images were compared with the images directly reconstructed using fixed trajectory. The framework was slightly modified by removing the trajectory optimization network and only training the end-to-end reconstruction U-Net using the standard super-

*Corresponding Author.

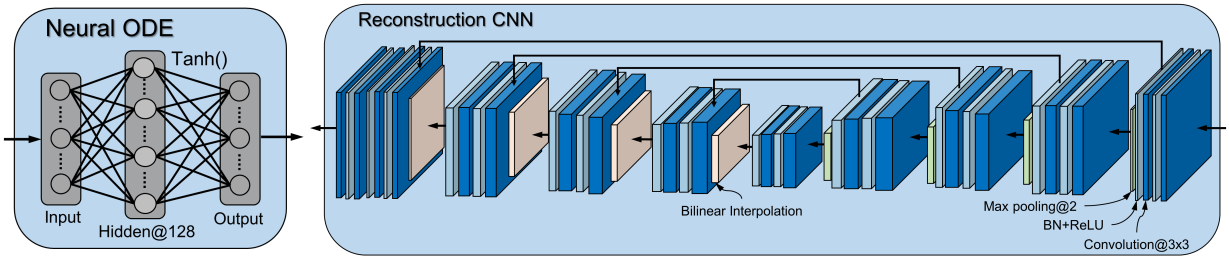

(a) Neural ODE (b) Reconstruction CNN

Figure 1. Schematic illustration of the proposed framework. **(a)** Detailed architecture of the neural ODE using a fully connected network. **(b)** A reconstruction CNN using a U-Net architecture.

vised learning approach. The qualitative evaluation of knee and brain images proves the improved image reconstruction using our proposed method. As illustrated in Figures 4, and 5, the reconstructed images from learned trajectories are consistently better than those from the fixed trajectories for each type. More specifically, Figure 4 provides an example of a reconstructed knee image using a learned Cartesian trajectory at an acceleration factor (AF) of 4.4. This figure shows that the learned trajectory provides better image features, improved image sharpness, and more detail recovery due to their optimized k-space coverage. The learned Cartesian trajectory outperformed the regular Cartesian trajectory at the same acceleration rate. Likewise, the learned spiral trajectories provided improved reconstruction performance compared to their fixed counterparts in Figure 5 for the brain images at the AXT1 sequence. Notably, the intermediate images directly obtained from the RSS reconstruction were shown at the top row of Figures 4, and 5 for the learned and fixed trajectories. It is evident that the learned trajectory can better remove structural and aliasing artifacts and provided more realistic image features and accurate image contrast than that of the fixed trajectory at the same level of acceleration, indicating the efficacy of the learning-based trajectory optimization.

We also explored the generalization ability of the proposed method to high acceleration level. Here, we undersampled the k-space data using only four spiral interleaves. As illustrated in Figure 6, the learned trajectory provides much sharper images and more image details than the fixed trajectory, of which the provided MR images are far away from satisfaction as the artifacts are very everywhere.

The context-awareness of the trajectory optimization is also investigated by comparing the optimized trajectories for datasets with different anatomies. Figure **??** illustrates the learned trajectories for brain and knee datasets, respectively, using an initialization of the same Cartesian trajectory. There are differences between the exemplified k-space for the brain and knee due to the difference of the imaged objects. The learned trajectories can realize this feature

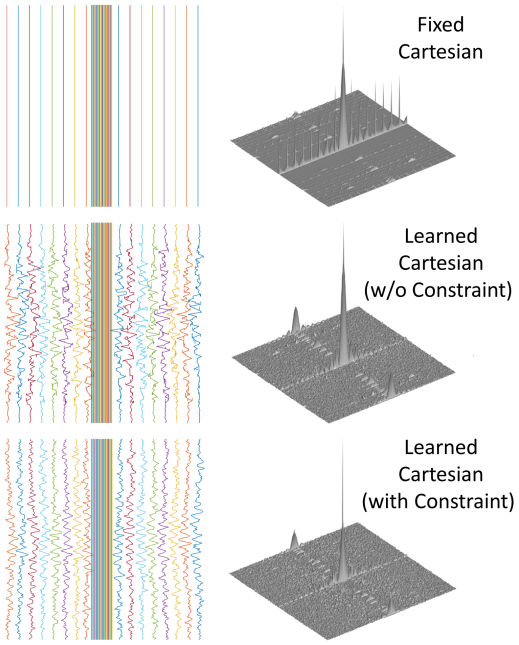

Figure 2. Trajectory comparison between fixed and learned Cartesian trajectory with acceleration factor AF = 6 (16 phase encoding lines) optimized on the knee datasets. **Top**: initial Cartesian trajectory. **Middle**: learned Cartesian trajectory without physical constraints. **Bottom**: learned Cartesian trajectory with physical constraints. The corresponding PSF is shown for each trajectory.

and correctly characterize the difference of the k-space density distribution. More specifically, the learned trajectory has more fluctuation and coverage for the scattered knee k-space than the more centralized brain k-space.

3. Segmentation on undersampled MRI

To further assess the clinical value of the proposed method, we apply it to the tumor segmentation task on undersampled MRI from the BraTS2020 [4] datatset. Here, the MRI is accelerated for 8-fold using radial trajectory. As illustrated in Fig. 7, the segmentation model will collapse

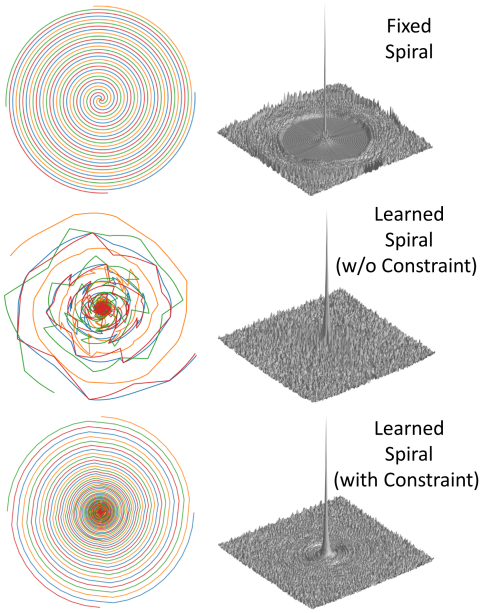

Figure 3. Trajectory comparison between fixed and learned spiral trajectory with 4 interleaves, optimized on the brain AXT1 datasets. **Top**: initial spiral trajectory. **Middle**: learned spiral trajectory without physical constraints. **Bottom**: learned spiral trajectory with physical constraints. The corresponding PSF is shown for each trajectory.

when directly training from the undersampled MRI (No-Recon). Using the proposed method, we can get a similar performance when compared to the model based on the fully sampled data. Our method is much more efficient as we accelerate it for eight times.

References

[1] Adam Paszke, S. Gross, Francisco Massa, A. Lerer, James Bradbury, Gregory Chanan, Trevor Killeen, Z. Lin, N. Gimelshein, L. Antiga, Alban Desmaison, Andreas Köpf, Edward Yang, Zach DeVito, Martin Raison, Alykhan Tejani, Sasank Chilamkurthy, B. Steiner, Lu Fang, Junjie Bai, and Soumith Chintala. Pytorch: An imperative style, high-performance deep learning library. In *NeurIPS*, 2019. 1

[2] Peter B Roemer, William A Edelstein, Cecil E Hayes, Steven P Souza, and Otward M Mueller. The nmr phased array. *Magnetic resonance in medicine*, 16(2):192–225, 1990. 1

[3] Olaf Ronneberger, Philipp Fischer, and Thomas Brox. U-net: Convolutional networks for biomedical image segmentation. In *MICCAI*, pages 234–241. Springer, 2015. 1

[4] Bjoern H. *et.al.* The multimodal brain tumor image segmentation benchmark (brats). *IEEE TMI*, 2015. 2, 6

[5] Chi-Ming Tsai and Dwight G Nishimura. Reduced aliasing artifacts using variable-density k-space sampling trajectories. *Magnetic Resonance in Medicine*, 43(3):452–458, 2000. 1

[6] Tomer Weiss, Ortal Senouf, Sanketh Vedula, Oleg Michailovich, Michael Zibulevsky, and Alex Bronstein. Pilot: Physics-informed learned optimal trajectories for accelerated mri. *arXiv preprint arXiv:1909.05773*, 2019. 1

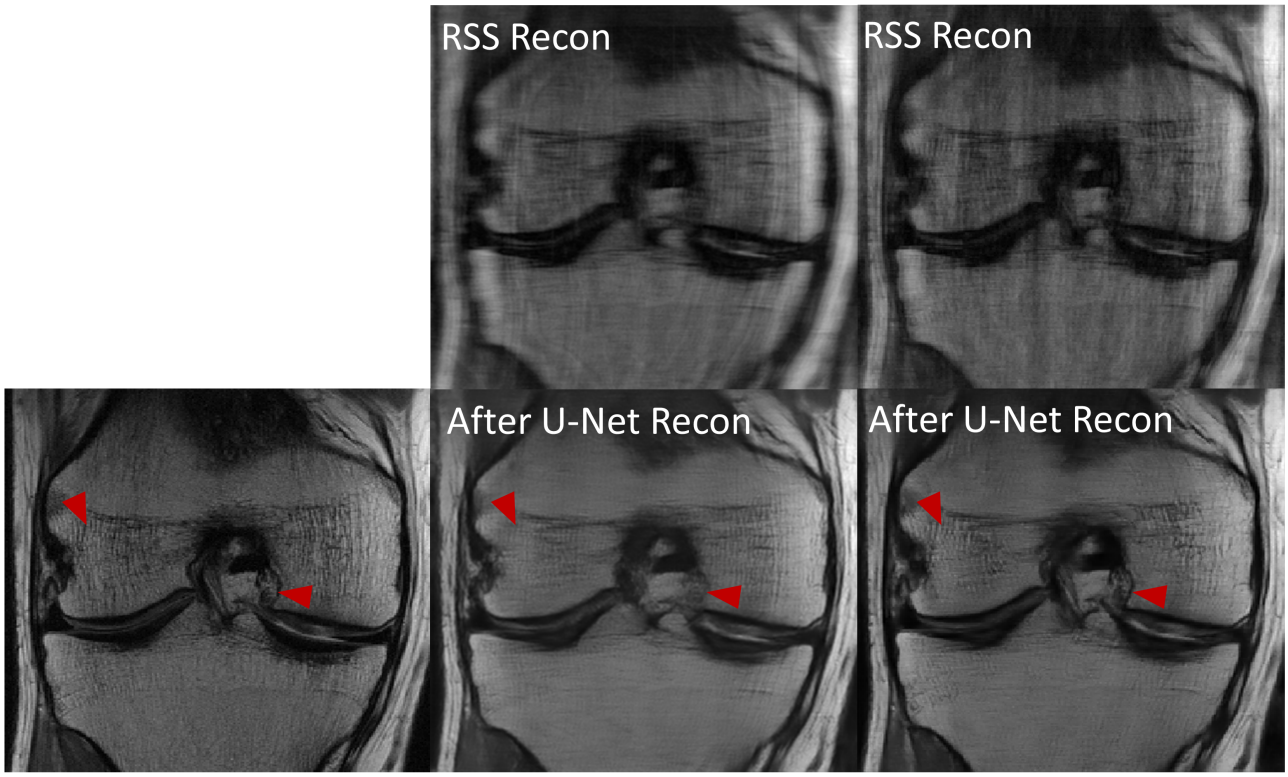

Figure 4. MRI reconstruction comparison between fixed and learned Cartesian trajectory at acceleration rate AF = 4.4 (32 phase encoding lines) for knee images. **Left column**: ground truth fully sampled image. **Middle column**: upper is the input image getting from RSS with fixed trajectory. Bottom is the reconstructed image from U-Net. **Right column**: upper is the input image getting from RSS with learned trajectory. Bottom is the reconstructed image from U-Net. The learned trajectory provides more realistic image feature recovery and sharper image quality than the fixed trajectory, as indicated by the red arrows.

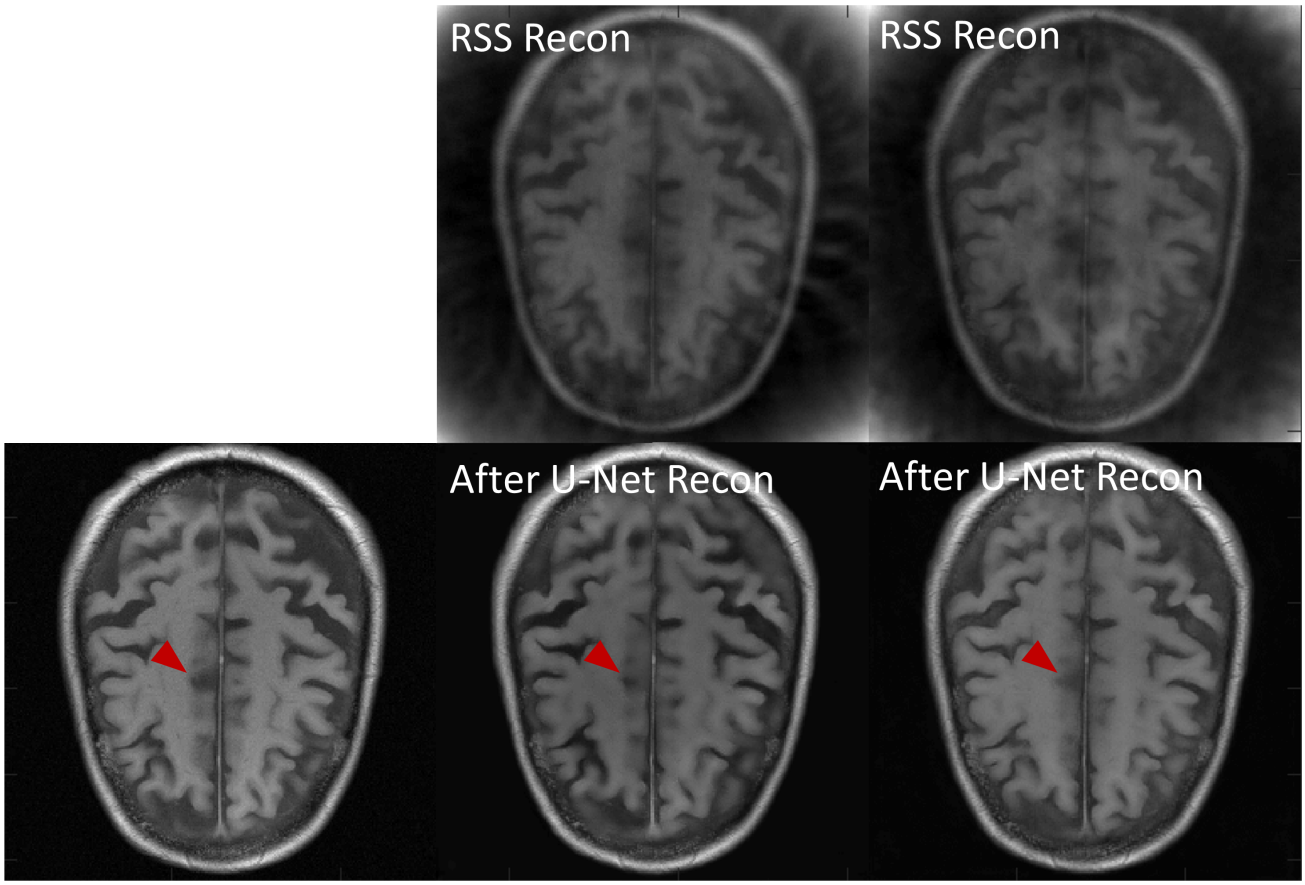

Figure 5. MRI reconstruction comparison between fixed and learned spiral trajectory with 16 interleaves for brain AXT1 images. **Left column**: ground truth fully sampled image. **Middle column**: upper is the input image getting from RSS with fixed trajectory. Bottom is the reconstructed image from U-Net. **Right column**: upper is the input image getting from RSS with learned trajectory. Bottom is the reconstructed image from U-Net. The learned trajectory provides sharper images and more image details than the fixed trajectory indicated by the red arrows.

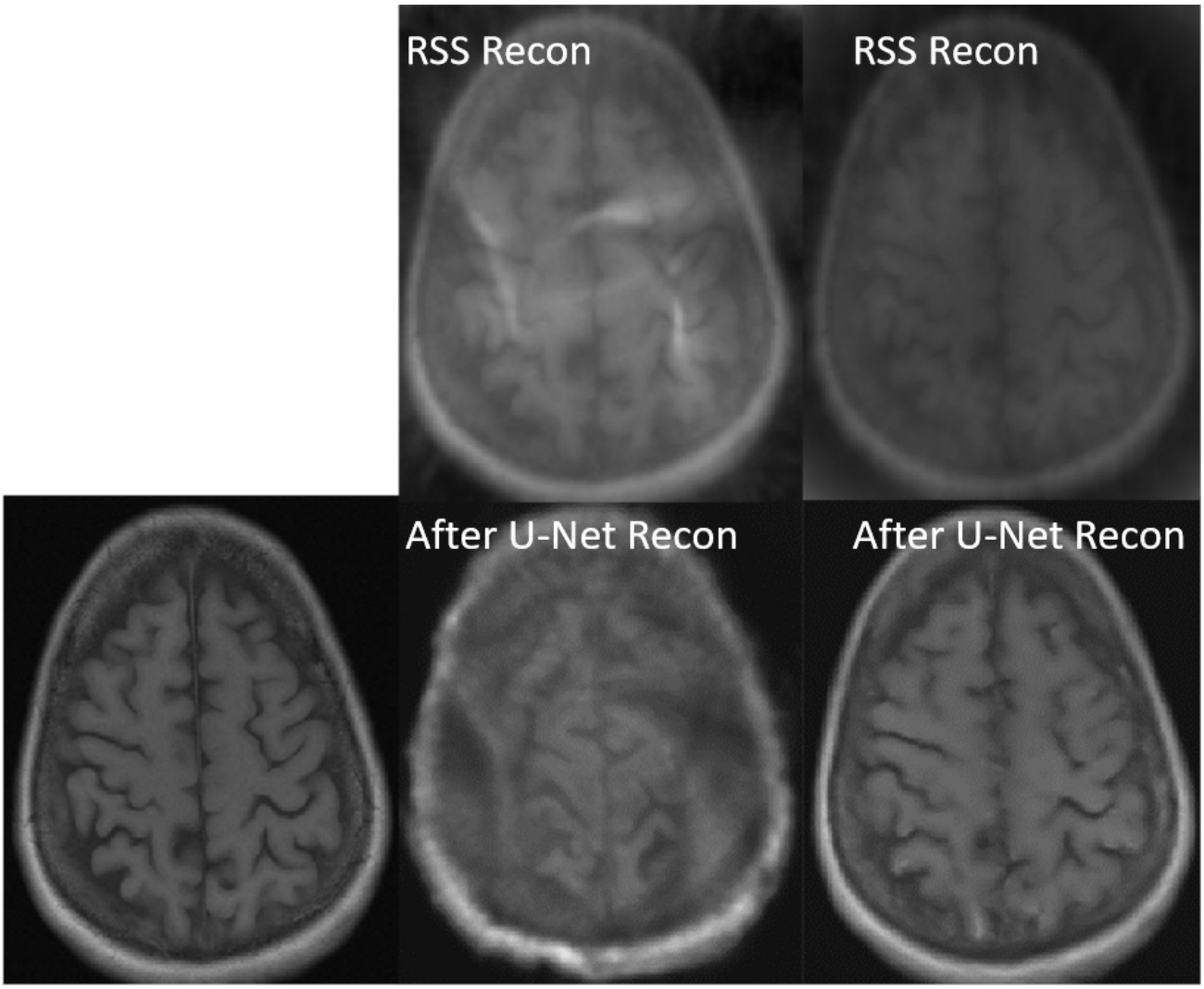

Figure 6. MRI reconstruction comparison between fixed and learned spiral trajectory with 4 interleaves for brain AXT1 images. **Left column**: ground truth fully sampled image. **Middle column**: upper is the input image getting from RSS with fixed trajectory. Bottom is the reconstructed image from U-Net. **Right column**: upper is the input image getting from RSS with learned trajectory. Bottom is the reconstructed image from U-Net. The learned trajectory provides sharper images and more image details than the fixed trajectory.

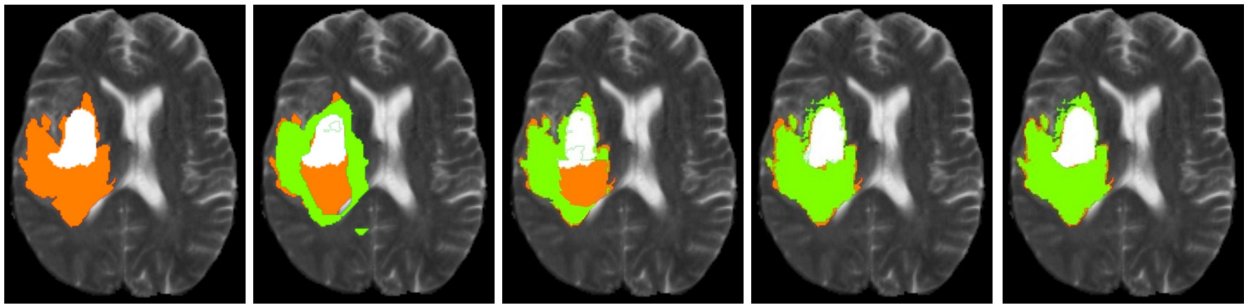

Figure 7. Tumor segmentation on BraTS2020 [4] dataset. The MRI is accelerated by 8-fold. Our method can provide a comparable segmentation result when compared to method using fully sampled MRI.